Synthesis and Crystal Structure of the Praseodymium Orthoborate λ-$PrBO_3$

Almut Haberer[a], Reinhard Kaindl[b], and Hubert Huppertz[a]

[a] Institut für Allgemeine, Anorganische und Theoretische Chemie, Leopold-Franzens-Universität Innsbruck, Innrain 52a, 6020 Innsbruck, Austria
[b] Institut für Mineralogie und Petrographie, Leopold-Franzens-Universität Innsbruck, Innrain 52, 6020 Innsbruck, Austria

Reprint requests to H. Huppertz. E-mail: Hubert.Huppertz@uibk.ac.at

Z. Naturforsch. **2010**, *65b,* 1206 – 1212; received May 18, 2010

The praseodymium orthoborate λ-$PrBO_3$ was synthesized from Pr_6O_{11}, B_2O_3, and PrF_3 under high-pressure / high-temperature conditions of 3 GPa and 800 °C in a Walker-type multianvil apparatus. The crystal structure was determined on the basis of single-crystal X-ray diffraction data, collected at room temperature. The title compound crystallizes in the orthorhombic aragonite-type structure, space group *Pnma*, with the lattice parameters $a = 577.1(2)$, $b = 506.7(2)$, $c = 813.3(2)$ pm, and $V = 0.2378(2)$ nm^3, with $R_1 = 0.0400$ and $wR_2 = 0.0495$ (all data). Within the trigonal-planar BO_3 groups, the average B–O distance is 137.2 pm. The praseodymium atoms are ninefold coordinated by oxygen atoms.

Key words: High Pressure, Crystal Structure, Multianvil, Orthoborate, Aragonite

Introduction

The rare earth orthoborates *RE*BO_3 exhibit a complex polymorphism. Besides structural ambiguities, the inconsistent nomenclature of the different polymorphs has made this class of borates even less transparent. According to the nomenclature of Meyer [1 – 3], the first polymorphs were designated with Greek letters; we will stick to this representation in this article, if possible. Depending on the size of the rare earth cations, orthoborate modifications with $CaCO_3$-related structures are known. While the phases β-*RE*BO_3 (*RE* = Sc, Er–Lu) [3 – 8] crystallize in the calcite-type structure, the borates λ-*RE*BO_3 (*RE* = La–Eu) [1, 9 – 11] adopt the aragonite-type structure. Furthermore, there are a low-temperature modification π-*RE*BO_3 (*RE* = Y, Nd–Lu) [7, 9] and a high-temperature modification μ-*RE*BO_3 (*RE* = Y, Sm–Gd, Dy–Lu) [12], which were suspected to have vaterite-related crystal structures [9]. In recent years, numerous studies concerning the structure and the space group of π- and μ-*RE*BO_3 were performed. Several hexagonal or rhombohedral space groups were proposed [12 – 16], as well as a monoclinic unit cell with pseudohexagonal stacking of the borate building blocks [17, 18]. The discussion is still in progress; at least, a consensus has been reached on the constitution of these borates from B_3O_9 groups for π-*RE*BO_3 (low-temperature phase), and from BO_3 groups for μ-*RE*BO_3 (high-temperature form). Two other high-temperature phases termed H-*RE*BO_3 (*RE* = La, Ce, Nd) [19, 20] with monoclinic crystal structures, and ν-*RE*BO_3 (*RE* = Ce–Nd, Sm–Dy) [1, 20 – 24] with triclinic crystal structures, are known. Additionally, high-pressure phases called χ-*RE*BO_3 (*RE* = Dy–Er) [25, 26] were synthesized.

Many of the orthoborates listed above were only obtained as powder samples, and some structural refinements were reported from powder diffraction data. For the case of λ-$PrBO_3$, only cell parameters were given by Meyer [1]. Another paper refers to the IR properties of λ-$PrBO_3$, without giving any structural details [27]. In this article, we present the first crystal structure determination of λ-$PrBO_3$ from single crystals obtained by high-pressure / high-temperature synthesis.

Experimental Section

Synthesis

According to Meyer, the synthesis of λ-$PrBO_3$ was first carried out under ambient pressure conditions by sintering B_2O_3 and Pr_6O_{11} at 1100 °C [1].

Single crystals of λ-$PrBO_3$ were now obtained under high-pressure / high-temperature conditions of 3 GPa

0932–0776 / 10 / 1000–1206 $ 06.00

and 800 °C. As the primary goal of the synthesis was a praseodymium fluoride borate, the starting reagents were Pr_6O_{11} (Strem Chemicals, 99.9 %), B_2O_3 (Strem Chemicals, 99.9+ %), and PrF_3 (Strem Chemicals, 99.9 %), which were ground together and filled into a boron nitride crucible (Henze BNP GmbH, HeBoSint® S100, Kempten, Germany) in the ratio $Pr_6O_{11} : B_2O_3 : PrF_3 = 11 : 6 : 27$. The boron nitride crucible was positioned inside the center of an 18/11 assembly, which was compressed by eight tungsten carbide cubes (TSM-10 Ceratizit, Reutte, Austria). A detailed description of the preparation of the assembly can be found in references [28 – 31]. The assembly was compressed to 3 GPa in 1.25 h, using a multianvil device, based on a Walker-type module and a 1000 t press (both devices from the company Voggenreiter, Mainleus, Germany). Having reached the reaction pressure, the sample was heated to 800 °C (cylindrical graphite furnace) in the following 10 min, kept there for 60 min, and cooled down to 600 °C within 20 min at constant pressure. After cooling down to r. t. by radiation heat loss, a decompression period of 3.75 h followed. A green crystalline sample could be separated from the surrounding boron nitride. Powder diffraction measurements showed that it consisted mainly of λ-$PrBO_3$, together with a praseodymium fluoride borate, which could not be fully characterized yet. Small green air- and water-resistant crystals of λ-$PrBO_3$ were mechanically separated from the product mixture.

IR spectroscopy

FTIR-ATR (*A*ttenuated *T*otal *R*eflection) spectra of the crystals were recorded with a Bruker Vertex 70 FT-IR spectrometer (resolution ∼ 0.5 cm^{-1}), attached to a Hyperion 3000 microscope in a spectral range from 600 – 4000 cm^{-1}. A frustrum-shaped germanium ATR-crystal with a tip diameter of 100 μm was pressed onto the surface of the crystals with a power of 5 N, which let them crush into pieces of μm-size. 64 scans for sample and background were acquired. Besides spectra correction for atmospheric influences, an enhanced ATR-correction [32], using the OPUS 6.5 software, was performed. A mean refraction index of the sample of 1.6 was assumed for the ATR-correction. Background correction and peak fitting followed *via* polynomial and folded Gaussian-Lorentzian functions.

Raman spectroscopy

Confocal Raman spectra of single crystals were obtained with a Horiba Jobin Yvon LabRam-HR 800 Raman microspectrometer. The sample was excited by the 532 nm emission line of a 30 mW Nd-YAG-laser under an Olympus 100× objective (numerical aperture = 0.9). The size and power of the laser spot on the surface were approximately 1 μm and 5 mW. The scattered light was dispersed by a grating with 1800 lines mm^{-1} and collected by a 1024 × 256 open electrode CCD detector. The spectral resolution, determined by measuring the Rayleigh line, was about 1.4 cm^{-1}. The polynomial and convoluted Gauss-Lorentz functions were applied for background correction and band fitting. The wavenumber accuracy of about 0.5 cm^{-1} was achieved by adjusting the zero-order position of the grating and regularly checked by a neon spectral calibration lamp.

Table 1. Crystal data and structure refinement for λ-$PrBO_3$.

Empirical formula	$PrBO_3$
Molar mass, g mol^{-1}	199.72
Crystal system	orthorhombic
Space group	*Pnma* (no. 62)
Powder diffractometer	Stoe Stadi P
Radiation; λ, pm	Mo$K_{\alpha1}$; 70.93
Powder diffraction data	
a, pm	576.3(2)
b, pm	506.3(1)
c, pm	812.7(2)
Volume, nm^3	0.2371(2)
Single-crystal diffractometer	Bruker AXS / Nonius Kappa CCD
Radiation; λ, pm	MoK_α; 71.073 (graphite monochromator)
Single-crystal data	
a, pm	577.1(2)
b, pm	506.7(2)
c, pm	813.3(2)
Volume, nm^3	0.2378(2)
Formula units per cell	$Z = 4$
Temperature, K	293(2)
Calculated density, g cm^{-3}	5.58
Crystal size, mm^3	0.03 × 0.03 × 0.025
Absorption coefficient, mm^{-1}	20.2
$F(000)$, e	352
θ range, deg	4.3 – 37.7
Range in *hkl*	±9, ±8, ±13
Total no. of reflections	3865
Independent reflections / R_{int}	687 / 0.0522
Reflections with $I \geq 2\sigma(I)$ / R_σ	579 / 0.0338
Data / ref. parameters	687 / 29
Absorption correction	Multi-scan (SCALEPACK [35])
Final indices R_1 / wR_2 [$I \geq 2\sigma(I)$]	0.0283 / 0.0467
Indices R_1 / wR_2 (all data)	0.0400 / 0.0495
Goodness-of-fit on F^2	1.098
Larg. diff. peak / hole, e $Å^{-3}$	2.00 / −1.73

Crystal structure analysis

The powder diffraction pattern of the sample was collected with a Stoe Stadi P diffractometer, using monochromatized Mo$K_{\alpha1}$ (λ = 70.93 pm) radiation. The main reflections of the powder pattern can be assigned to λ-$PrBO_3$ (Fig. 1), while additional reflections belong to a not yet fully characterized praseodymium fluoride borate. The diffraction pattern of λ-$PrBO_3$ was indexed with the program ITO [33] on the basis of an orthorhombic unit cell. The lattice parameters

Table 2. Atomic coordinates and isotropic equivalent displacement parameters U_{eq} (Å^2) for λ-$PrBO_3$ (space group *Pnma*). U_{eq} is defined as one third of the trace of the orthogonalized U_{ij} tensor.

Atom	W. position	*x*	*y*	*z*	U_{eq}
Pr	4*c*	0.24225(4)	¼	0.58450(3)	0.00638(9)
B	4*c*	0.0841(9)	¼	0.2382(7)	0.0073(8)
O1	4*c*	0.0958(6)	¼	0.0696(4)	0.0107(7)
O2	8*d*	0.0864(5)	0.0165(5)	0.3231(3)	0.0099(5)

Table 3. Anisotropic displacement parameters U_{ij} (Å^2) for λ-$PrBO_3$ (space group *Pnma*).

Atom	U_{11}	U_{22}	U_{33}	U_{23}	U_{13}	U_{12}
Pr	0.0065(2)	0.0065(2)	0.0062(2)	0	0.00039(9)	0
B	0.007(2)	0.009(2)	0.006(2)	0	0.000(2)	0
O1	0.012(2)	0.013(2)	0.008(2)	0	−0.000(2)	0
O2	0.011(2)	0.008(2)	0.011(2)	0.0008(9)	−0.0018(9)	−0.0006(9)

Table 4. Interatomic distances (pm) and angles (deg), calculated with the single-crystal lattice parameters of λ-$PrBO_3$ with standard deviations in parentheses.

Pr–O1a	239.5(4)	B–O1	137.3(7)
Pr–O2a (2×)	244.7(3)	B–O2 (2×)	137.0(4)
Pr–O2b (2×)	256.3(3)		
Pr–O2c (2×)	259.4(3)	O1–B–O2 (2×)	120.2(2)
Pr–O1b (2×)	270.3(2)	O2–B–O2	119.5(4)

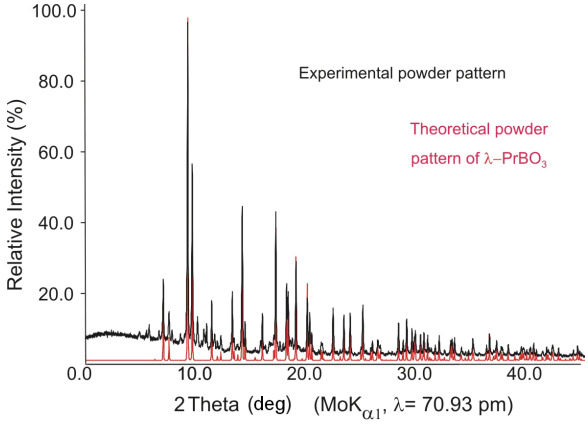

Fig. 1 (color online). Experimental powder pattern of the sample in comparison to the theoretical powder pattern of λ-$PrBO_3$ underneath, based on single-crystal diffraction data. Additional reflections of the sample are caused by a praseodymium fluoride borate not fully characterized yet.

a = 576.3(2), *b* = 506.3(1), and *c* = 812.7(2) pm (Table 1) were gained from least-squares fits of the powder data. The correct indexing of the pattern was confirmed by intensity calculations [34], taking the atomic positions from the single-crystal structure refinements of λ-$PrBO_3$ (Table 2). The data are in good agreement with Meyer's parameters (*a* = 576.9, *b* = 506.1, and *c* = 812.9 pm) [1] and with the single-crystal data (*a* = 577.1(2), *b* = 506.7(2), and *c* = 813.3(2) pm).

For the crystal structure analysis, small single crystals of λ-$PrBO_3$ were isolated by mechanical fragmentation and measured with an Enraf-Nonius Kappa CCD with graphite-monochromatized MoK_α (λ = 71.073 pm) radiation. Afterwards, a multi-scan absorption correction was applied to the data (SCALEPACK [35]). According to the systematic extinctions, the space groups $Pn2_1a$ (no. 33) and *Pnma* (no. 62) were derived. Structure solution and parameter refinement (full-matrix least-squares against F^2) were successfully performed in *Pnma*, using the SHELX-97 software suite [36, 37] with anisotropic displacement parameters for all atoms. All relevant details of the data collection and evaluation are listed in Table 1. The final difference Fourier synthesis did not reveal any significant residual peaks. Additionally, the positional parameters (Table 2), anisotropic displacement parameters (Table 3), interatomic distances, and angles (Table 4) are listed below.

Further details of the crystal structure investigation may be obtained from Fachinformationszentrum Karlsruhe, 76344 Eggenstein-Leopoldshafen, Germany (fax: +49-7247-808-666; e-mail: crysdata@fiz-karlsruhe.de, http://www.fiz-informationsdienste.de/en/DB/icsd/depot_anforderung.html) on quoting the deposition number CSD-421745.

Results and Discussion

λ-$PrBO_3$ crystallizes in an aragonite-type structure (space group *Pnma*), as predicted from powder diffraction data by Meyer [1]. The structure is composed of praseodymium atoms and isolated trigonal-planar BO_3 units (Fig. 2). Viewing along [100], the BO_3 groups are stacked in channels, surrounded by hexagonally arranged praseodymium cations in an antiprismatic arrangement, which is slightly off-centered, so that the boron atoms are incongruent (Fig. 3). The B–O bond lengths of the BO_3 groups of 137.0(4)

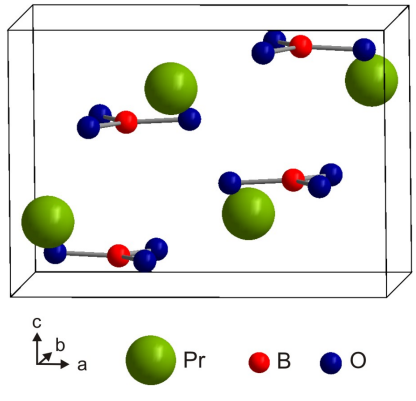

Fig. 2 (color online). Schematic drawing of the unit cell of λ-$PrBO_3$ with trigonal-planar BO_3 units.

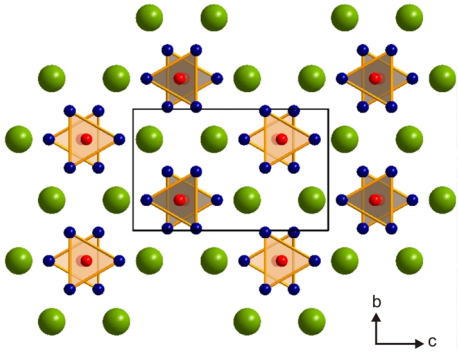

Fig. 3 (color online). View of the λ-$PrBO_3$ structure along [100]. The BO_3 groups are stacked in channels formed by hexagonally arranged praseodymium cations in a slightly off-centered antiprismatic arrangement.

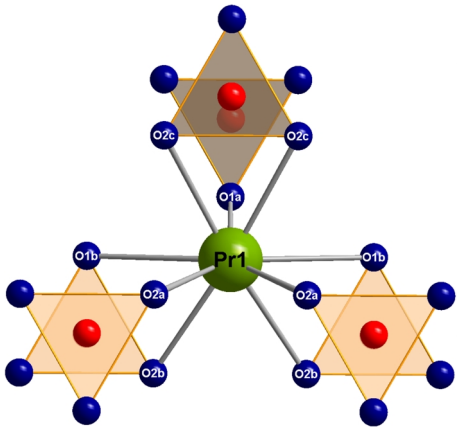

Fig. 4 (color online). Coordination sphere of the praseodymium cation in λ-$PrBO_3$. Six surrounding BO_3 groups donate either one or two oxygen atoms, leading to a ninefold coordination.

and 137.3(7) pm are typical for threefold coordinated boron and agree with the distances ascertained for λ-$NdBO_3$ (137.5 pm) [11]. The O–B–O angles are 119.5(4) and 120.2(2)°, as expected for a trigonal-planar geometry. Müller-Bunz *et al.* observed a 5.6 pm dislocation of the boron atom from the plane spanned by its oxygen ligands in λ-$NdBO_3$ [11]. For λ-$PrBO_3$, this value is reduced to 3.2 pm.

There is one crystallographically unique praseodymium atom in the structure. Six surrounding BO_3 groups donate either one or two oxygen atoms, leading to a ninefold coordination sphere of praseodymium (Fig. 4). The Pr–O distances are in the range between 239.5(4) and 270.3(2) pm, which is in agreement with the bond lengths of ninefold coordinated praseodymium in HP-PrO_2 (235.9(2) to 283.7(3) pm) [38]. As expected from the smaller ionic radius of Nd^{3+} (130.3 pm) in comparison to Pr^{3+} (131.9 pm), the corresponding bond lengths in the isotypic phase λ-$NdBO_3$ are slightly shorter (238.6 to 269.3 pm) [11].

The calculation of the bond-valence sums for λ-$PrBO_3$ with the bond-length / bond-strength (BLBS) concept (VALIST: Bond Valence Calculation and Listing [39]) and the CHARDI concept (*char*ge *di*stribution in solids according to Hoppe [40]) confirmed the formal ionic charges resulting from the single-crystal structure analysis (Σ*V* (BLBS): +3.02 (Pr), +3.00 (B), −1.93 (O1), −2.05 (O2) and Σ*Q* (CHARDI): +3.00 (Pr), +3.00 (B), −1.89 (O1), −2.05 (O2).

Furthermore, we calculated the MAPLE value (*Ma*delung *P*art of *L*attice *E*nergy according to Hoppe [41 – 43]) of λ-$PrBO_3$ in order to compare it with the sum of the MAPLE values for the high-pressure modification of Pr_2O_3 [44] and the ambient-pressure modification B_2O_3-I [45] [0.5 Pr_2O_3 (3457 kcal mol^{-1}) +0.5 B_2O_3-I (5237 kcal mol^{-1})]. The calculated value (4318 kcal mol^{-1}) for λ-$PrBO_3$ and the MAPLE value obtained from the sum of the binary oxides (4347 kcal mol^{-1}) tally well (deviation 0.7 %) and confirm the value of 4318 kcal mol^{-1} for the isotypic compound λ-$NdBO_3$ [11].

IR spectroscopy

Fig. 5 shows the FTIR-ATR spectrum of λ-$PrBO_3$ single crystals in the range between 600 – 1600 cm^{-1}. The IR absorption bands for aragonite-type orthoborates have been well discussed in the literature and can be divided into four different absorption areas: an in-

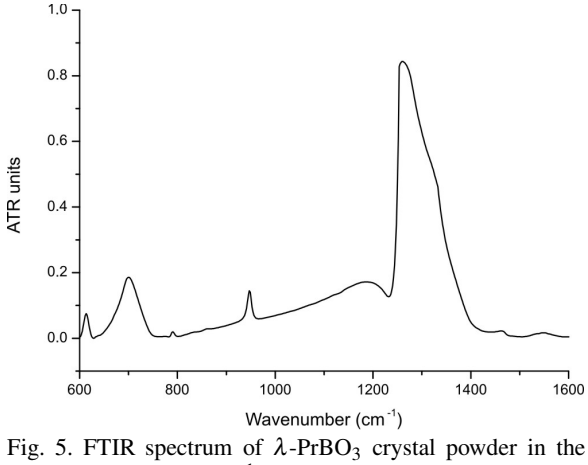

Fig. 5. FTIR spectrum of λ-$PrBO_3$ crystal powder in the range of 600 – 1600 cm^{-1}.

Table 5. Wavenumbers and possible assignment of ATR-FTIR absorption bands in the spectrum of λ-$PrBO_3$ single crystals (left) and of absorption bands reported from the bulk material [48].

Band	Single crystal IR Assignment	Bulk IR [48] Band
629	ν_4	590, 610
700	ν_2	713
790		788
1190	ν_1	944
1260		1250, 1285
1463	ν_3	

plane bending (ν_4) of the BO_3 groups results in bands between 600 and 670 cm^{-1}, out-of-plane bending (ν_2) occurs near 740 cm^{-1}, symmetric stretching modes (ν_1) between 940 and 1000 cm^{-1}, and asymmetric stretching vibrations (ν_3) between 1300 – 1500 cm^{-1} [46, 47]. Bulk IR measurements of λ-$PrBO_3$ were previously performed by Laperches *et al.* [48]. Since their band assignment is not in agreement with the literature, Table 5 compares the positioning of the bands of bulk and single crystal λ-$PrBO_3$, but labels the absorption modes as shown above. There is good agreement between the absorptions of the FTIR-ATR spectrum of λ-$PrBO_3$ single crystals and the literature data. A comparable pattern of absorption bands is reported for aragonite ($CaCO_3$) [49].

Raman spectroscopy

The Raman spectrum of the λ-$PrBO_3$ single crystals shows several intense bands below 500 cm^{-1} (Fig. 6), which can be assigned to the *RE*–O bond bending and stretching vibrations, as well as to the lattice vibrations (Table 6). For aragonite ($CaCO_3$), also a large number of external Raman-active modes are reported below 500 cm^{-1} [49]. The bands observed between 600 and 700 cm^{-1} for λ-$PrBO_3$, correspond to the pulse vibration modes of $CaCO_3$ between 700 and 720 cm^{-1} (ν_4 modes). The bands around 900 cm^{-1} in borates are usually assigned to the stretching modes of BO_4 tetrahedra, whereas BO_3 groups are expected > 1100 cm^{-1} [50 – 55]. Nevertheless, the most intense single band of λ-$PrBO_3$ occurs at 950 cm^{-1} and is also observed in the BO_3 group-containing phases $RE_5(BO_3)_2F_9$ (*RE* = Er, Yb) [56]. Aragonite-structured $CaCO_3$ shows it's most intense band at 1085 cm^{-1}, which is owed to the symmetric stretching vibration of the CO_3 group (ν_1 mode) [49]. Above 1200 cm^{-1}, several broader bands for λ-$PrBO_3$ are observed and assigned to the asymmetric stretching vibrations (ν_3) of the BO_3 groups [53]. In classical aragonite, these modes appear at higher wavenumbers.

Table 6. Wavenumbers and possible assignment of Raman bands in the spectrum of λ-$PrBO_3$.

Band	Assignment	Band	Assignment
106		596	
113		607	pulse vibration
121		631	of BO_3
143		694	
180	Lattice, Pr–O,	950	symmetric stretching ?
193	bending/stretching	1240	
227	of BO_3	1242	asymmetric
252		1260	stretching of
330		1270	BO_3
373		1383	

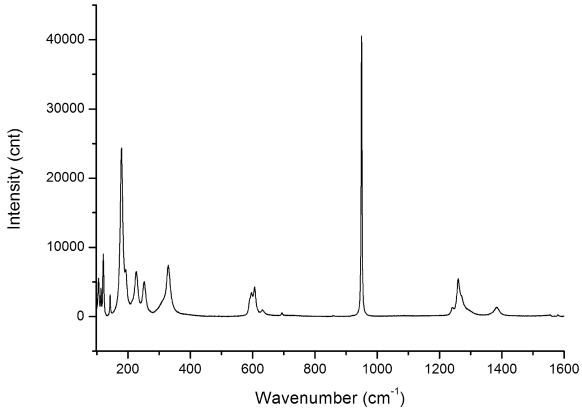

Fig. 6. Raman spectrum of a single crystal of λ-$PrBO_3$ in the range of 100 – 1600 cm^{-1}.

Conclusions

Under normal pressure conditions, glasses and powders are often the favored products of reactions in oxoborate chemistry. As demonstrated in this paper, high-pressure / high-temperature conditions can enforce the formation of a crystalline product, allowing the first single-crystal structure determination of λ-$PrBO_3$. Starting materials for the synthesis of λ-$PrBO_3$ were Pr_6O_{11}, B_2O_3, and PrF_3, resulting in a not yet fully characterized praseodymium fluoride borate as a side product. The formation of borates under the applied high-pressure / high-temperature conditions is often observed; they seem to be the most favorable reaction product even in the presence of rare earth fluorides. In these cases, the fluoride does either not participate in the reaction or humidity seems to lead to the

formation of gaseous HF. An impact on the formation and stability range of the obtained borates has not been observed so far, the same reaction products occur without the fluoride.

Acknowledgements

We thank Dr. G. Heymann for collecting the single-crystal data. This work was financially supported by the Deutsche Forschungsgemeinschaft (HU966/2-3).

[1] H. J. Meyer, *Naturwissenschaften* **1969**, *56*, 458.
[2] H. J. Meyer, *Naturwissenschaften* **1972**, *59*, 215.
[3] H. J. Meyer, A. Skokan, *Naturwissenschaften* **1971**, *58*, 566.
[4] D. A. Keszler, H. Sun, *Acta Crystallogr.* **1988**, *C44*, 1505.
[5] H. Huppertz, *Z. Naturforsch*. **2001**, *56b*, 697.
[6] S. C. Abrahams, J. L. Bernstein, E. T. Keve, *J. Appl. Crystallogr.* **1971**, *4*, 284.
[7] S. Hosokawa, Y. Tanaka, S. Iwamoto, M. Inoue, *J. Mater. Sci.* **2008**, *43*, 2276.
[8] T. A. Bither, H. S. Young, *J. Solid State Chem.* **1973**, *6*, 502
[9] E. M. Levin, R. S. Roth, J. B. Martin, *Am. Mineral.* **1961**, *46*, 1030.
[10] J. Weidelt, H. U. Bambauer, *Naturwissenschaften* **1968**, *55*, 342.
[11] H. Müller-Bunz, T. Nikelski, Th. Schleid, *Z. Naturforsch.* **2003**, *58b*, 375.
[12] R. E. Newnham, M. J. Redman, R. P. Santoro, *J. Am. Ceram. Soc*. **1963**, *46*, 253.
[13] W. F. Bradley, D. L. Graf, R. S. Roth, *Acta Crystallogr*. **1966**, *20*, 283.
[14] G. Chadeyron, M. El-Ghozzi, R. Mahiou, A. Arbus, J. C. Cousseins, *J. Solid State Chem.* **1997**, *128*, 261.
[15] M. Ren, J. H. Lin, Y. Dong, L. Q. Yang, M. Z. Su, L. P. You, *Chem. Mater.* **1999**, *11*, 1576.
[16] M. Th. Cohen-Adad, Ch. Kappenstein, O. Aloui-Lebbou, C. Goutaudier, G. Panczer, C. Dujardin, C. Pedrini, P. Florian, D. Massiot, F. Gerard, *J. Solid State Chem.* **2000**, *154*, 204.
[17] P. E. D. Morgan, P. J. Carroll, F. F. Lange, *Mater. Res. Bull.* **1977**, *12*, 251.
[18] J. H. Lin, S. Sheptyakov, Y. Wang, P. Allenspach, *Chem. Mater.* **2004**, *16*, 2418.
[19] R. Böhlhoff, H. U. Bambauer, W. Hoffmann, *Naturwissenschaften* **1970**, *57*, 129.
[20] R. Böhlhoff, H. U. Bambauer, W. Hoffman, *Z. Kristallogr*. **1971**, *133*, 386.
[21] K. K. Palkina, V. G. Kuznetsov, L. A. Butman, B. F. Dzhurinskii, *Acad. Sci. USSR* **1976**, *2*, 286.
[22] S. Noirault, O. Joubert, M. T. Caldes, Y. Piffard, *Acta Crystallogr.* **2006**, *E62*, i228.
[23] G. Corbel, M. Leblanc, E. Antic-Fidancev, M. Lemaître-Blaise, J. C. Krupa, *J. Alloys Compd*. **1999**, *287*, 71.
[24] H. Emme, H. Huppertz, *Acta Crystallogr.* **2004**, *C60*, i117.
[25] H. Huppertz, B. von der Eltz, R.-D. Hoffmann, H. Piotrowski, *J. Solid State Chem.* **2002**, *166*, 203.
[26] H. Huppertz, unpublished results.
[27] J. P. Laperches, P. Tarte, *Spectrochim. Acta* **1966**, *22*, 120.
[28] V. F. Ross, J. O. Edwards, *The Structural Chemistry of the Borates*, Wiley, New York, **1967**.
[29] D. Walker, M. A. Carpenter, C. M. Hitch, *Am. Mineral.* **1990**, *75*, 1020.
[30] D. Walker, *Am. Mineral.* **1991**, *76*, 1092.
[31] H. Huppertz, *Z. Kristallogr.* **2004**, *219*, 330.
[32] F. M. Mirabella, Jr. (ed.), *Internal Reflection Spectroscopy, Theory and Applications*, Marcel Dekker, New York **1992**, p. 276.
[33] J. W. Visser, *J. Appl. Crystallogr.* **1969**, *2*, 89.
[34] WINX^{POW} Software, Stoe & Cie GmbH, Darmstadt (Germany) **1998**.
[35] Z. Otwinowski, W. Minor in *Methods in Enzymology*, Vol. 276, *Macromolecular Crystallography*, Part A (Eds.: C. W. Carter, Jr., R. M. Sweet), Academic Press, New York, **1997**, pp. 307.
[36] G. M. Sheldrick, SHELXS-97 and SHELXL-97, Program Suite for the Solution and Refinement of Crystal Structures, University of Göttingen, Göttingen (Germany) **1997**.
[37] G. M. Sheldrick, *Acta Crystallogr.* **1990**, *A46*, 467; *ibid.* **2008**, *A64*, 112.
[38] A. Haberer, H. Huppertz, *Z. Anorg. Allg. Chem.* **2010**, *636*, 363.
[39] A. S. Wills, VALIST (version 3.0.13), University College, London (U. K.), **1998 – 2008**. Program available from: www.ccp14.ac.uk.
[40] R. Hoppe, S. Voigt, H. Glaum, J. Kissel, H. P. Müller, K. J. Bernet, *J. Less-Common Met.* **1989**, *156*, 105.
[41] R. Hoppe, *Angew. Chem.* **1966**, *78*, 52; *Angew. Chem., Int. Ed. Engl.* **1966**, *5*, 96.
[42] R. Hoppe, *Angew. Chem.* **1970**, *82*, 7; *Angew. Chem., Int. Ed. Engl.* **1970**, *9*, 25.
[43] R. Hübenthal, M. Serafin, R. Hoppe, MAPLE (version 4.0), Program for the Calculation of Distances, Angles, Effective Coordination Numbers, Coordination Spheres, and Lattice Energies, University of Gießen, Gießen (Germany) **1993**.

[44] L. Eyring, N. C. Baenziger, *J. Appl. Phys.* **1962**, *33*, 428.
[45] G. E. Gurr, P. W. Montgomery, C. D. Knutson, B. T. Gorres, *Acta Crystallogr.* **1970**, *B26*, 906.
[46] C. E. Weir, R. A. Schroeder, *J. Research NBS-A, Phys. Chem. A* **1964**, *68*, 465.
[47] J. H. Denning, S. D. Ross, *Spectrochim. Acta* **1971**, *A28*, 1775.
[48] J. P. Laperches, P. Tarte, *Spectrochim. Acta* **1966**, *22*, 1201.
[49] R. Frech, E. C. Wang, J. B. Bates, *Spectrochim. Acta* **1980**, *A36*, 915.
[50] G. Corbel, R. Retoux, M. Leblanc, *J. Solid State Chem.* **1998**, *139*, 52.
[51] H. Huppertz, *J. Solid State Chem.* **2004**, *177*, 3700.
[52] G. Chadeyron, M. El-Ghozzi, R. Mahiou, A. Arbus, J. C. Cousseins, *J. Solid State Chem.* **1997**, *128*, 261.
[53] L. Jun, X. Shuping, G. Shiyang, *Spectrochim. Acta* **1995**, *A51*, 519.
[54] J. C. Zhang, Y. H. Wang, X. Guo, *J. Lumin.* **2007**, *122 – 123*, 980.
[55] G. Padmaja, P. Kistaiah, *J. Phys. Chem.* **2009**, *A113*, 2397.
[56] A. Haberer, R. Kaindl, J. Konzett, R. Glaum, H. Huppertz, *Z. Anorg. Allg. Chem.* **2010**, *636*. 1326.